Electromechanical and Electromagnetic Simulation of RF-MEMS Complex Networks Based on Compact Modeling Approach

J. Iannacci*, A. Faes*, T. Kuenzig**, M. Niessner** and G. Wachutka**

*Fondazione Bruno Kessler – FBK, MEMS Research Unit,
Via Sommarive 18, 38123, Povo – Trento, Italy, iannacci@fbk.eu
**Munich University of Technology, Institute for Physics of Electrotechnology, Munich, Germany

ABSTRACT

This work reports the coupled electromechanical and electromagnetic simulation of an RF-MEMS complex network, i.e. a reconfigurable power attenuator for RF signals. The network exploits 3 Poly-Silicon resistive loads that can be independently selected or shorted by means of electrostatically actuated MEMS switches and, thus, change the attenuation level of the RF signal. The network is simulated by exploiting a MEMS compact model library previously developed by the authors in the VerilogA© programming language. The tool enables the fast simulation both of the electromechanical characteristic of the switches as well as of the RF behavior of the whole network. The simulated results are compared to the measured pull-in/pull-out characteristic of the switch and measured S-parameters, proving the good predictive capabilities achieved by the compact model library. The proposed method appears to be a sound solution for the fast simulation of RF-MEMS complex networks, particularly desirable in the design phase.

Keywords: RF-MEMS, coupled simulation, compact modeling, complex network.

1 INTRODUCTION

RF-MEMS (MicroElectroMechanical-Systems for Radio Frequency applications) technology has been drawing the attention of the scientific community in the last 15 years because it enables the fabrication of high-performance and low-cost passive components. High Q-factor and low-loss variable capacitors [1], inductors [2] and microswitches [3] in RF-MEMS technology have been presented and discussed in literature. Their availability enables the fabrication of complex functional sub-blocks for telecommunication systems, where several of such elemental passives are employed. Significant examples of RF-MEMS-based complex networks are reconfigurable impedance matching networks [4], tuning filters [5], phase shifters [6] and switching units [7], and their availability can improve the performance of the entire systems comprising them [8].

In this work, we face the issue of predicting the behavior of RF-MEMS-based complex networks through an ad-hoc simulation approach. Such an aspect is not fully straightforward as MEMS devices always involve the coupling of different physical domains and magnitudes that have to be managed together by the simulator software. In particular, in the case of interest here discussed (i.e. RF-MEMS) the mechanical, electrical and electromagnetic domains are involved.

The proposed approach relies on a MEMS model library previously developed by the authors in the VerilogA© programming language for the Cadence© IC development framework [9,10]. The case study of this paper refers to a MEMS-based reconfigurable RF power attenuator and discusses the methodology to exploit the compact model library. The good accuracy in predicting the mixed-domain behavior of the RF attenuator proves that the proposed simulation methodology can be exploited for the fast simulation of RF-MEMS complex topologies with multiple degrees of freedom (dofs).

2 THE RF-MEMS RECONFIGURABLE POWER ATTENUATOR

The microphotograph of the RF-MEMS multi-state power attenuator is shown in Fig. 1 and has been already presented and discussed in [11].

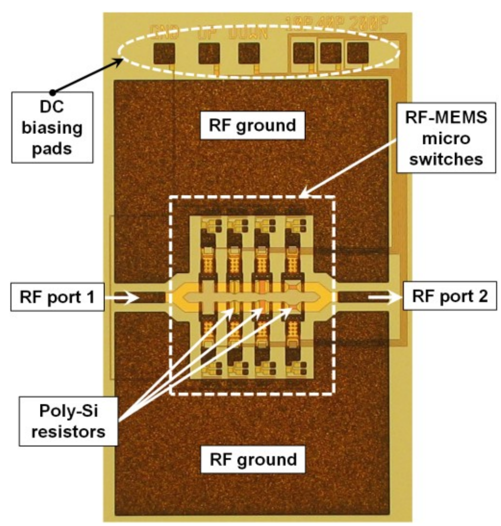

Figure 1: Microphotograph of the MEMS-based reconfigurable RF power attenuator. The Poly-Silicon resistive loads, selection microswitches and DC pads to control them are highlighted.

The network features 3 Poly-Silicon resistors loading the RF line, that can be selectively inserted or shorted by means of ohmic series microswitches (visible in figure), and, thus, reconfigure the RF signal attenuation level realized by the network. With 4 switching stages the network realizes $2^4 = 16$ different attenuation levels.

3 ELECTROMECHANICAL SIMULATION

This section discusses the coupled electromechanical simulation of the MEMS switch design employed in the complete network. Fig. 2-top shows the 3D profile of a microswitch obtained with a White Light Interferometer – WLI (WYKO NT1100 by Veeco).

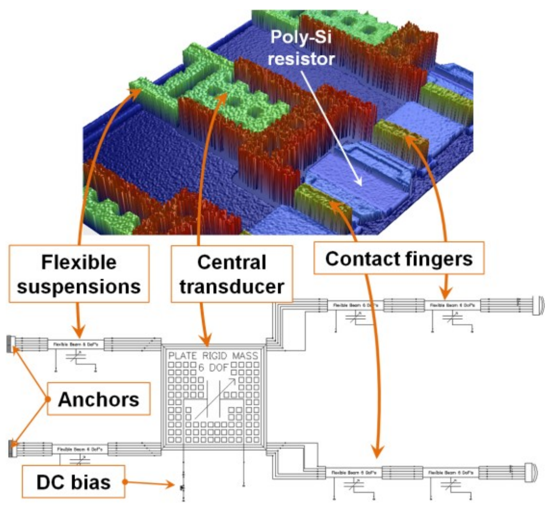

Figure 2: *Top-image*. 3D view of the MEMS cantilever-type microswitch acquired with the White Light Interferometer (WLI). *Bottom-image*. Cadence schematic of the switch assembled with the elemental components available in the MEMS compact model library.

The switch is hinged only at one end (i.e. cantilever), while the contact fingers on the other end short the underlying resistance when the microrelay is actuated (i.e. pulled-in). The central rigid Gold plate realizes the electromechanical transducer. Fig. 2-bottom shows the Cadence schematic of the switch composed of the elemental models available in the VerilogA© library, ready to be simulated with the Spectre© circuit simulator.

The measured (WLI) and simulated (Spectre DC simulation) pull-in/pull-out characteristic of the switch is reported in Fig. 3. The pull-in and pull-out transitions, measured at +28 V and +23 V for positive applied bias, and at -24 V and -19 V for negative applied bias, respectively, are accurately predicted by Spectre. A right-hand rigid shift of the whole experimental characteristic is visible. This is due to the charge injected in the insulating layer between the movable MEMS membrane and the underlying fixed electrode during the measurement [12]. Such an unwanted charge builds a spurious DC voltage opposed to the applied controlling voltage, indeed reducing the actual voltage applied to the MEMS switch. The charge accumulation is a phenomenon affecting basically all electrostatically controlled MEMS/RF-MEMS devices, and its inclusion in the simulations cannot be neglected, if a certain predictive accuracy is desired.

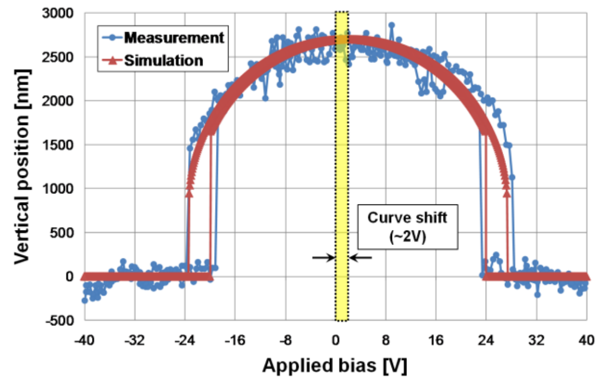

Figure 3: Experimental and simulated pull-in/pull-out characteristic of the MEMS switch of Fig. 2. The curve shift due to the charge entrapped in the insulator is visible.

This effect has been accounted for in the simulation by cascading to the voltage source defining the DC bias (V_{bias}) a negative DC level (V_{charge}), due to the entrapped charge, equal to 2 V. A close-up of the schematic of Fig. 2-bottom is reported in Fig. 4, and the effective voltage applied to the MEMS switch is equal to V_{bias} - V_{charge}.

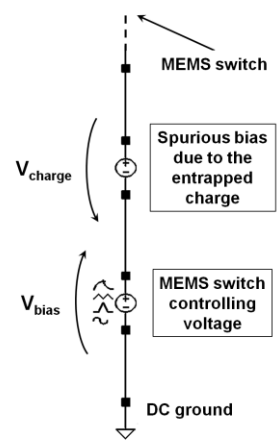

Figure 4: Close-up of the schematic in Fig. 2-bottom showing the voltage source providing the DC bias to the MEMS switch, and the additional voltage source accounting for the spurious bias induced by the charge entrapped in the insulator. The effective voltage applied to the MEMS switch is equal to V_{bias} - V_{charge}.

To conclude the section on the electromechanical simulation of the MEMS ohmic switch, its dynamic behavior is also simulated (transient simulation in Spectre). A 250 Hz, 0-40 V pulse (ON for 800 μs), is applied to the schematic of Fig. 2-bottom. The vertical displacement characteristic of the switch is reported in Fig. 5. The two close-ups, in the figure right-hand side, show the bouncing after the landing of the switch on the underlying contact pads, as well as the damped ringing after release. The squeeze film damping effect, that causes the damping on the ringing after release, is accounted for in the MEMS compact model library, and relies on a modified Reynolds equation as reported in [13].

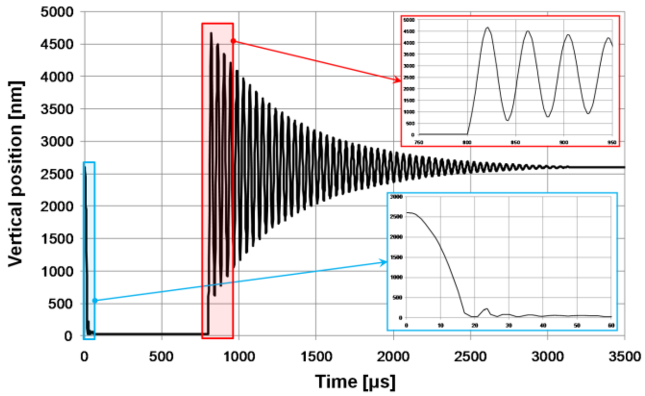

Figure 5: Dynamic response (transient simulation in Spectre) of the switch of Fig. 2, when a square pulse (0-40 V, ON for 800 µs) is applied. Close-ups for the actuation and release transitions are visible.

4 COUPLED ELECTROMECHANICAL AND ELECTROMAGNETIC SIMULATION

This section focuses on the coupled electromechanical and electromagnetic simulation of the entire RF-MEMS multi-state power attenuator discussed here, and its schematic assembled within Cadence is depicted in Fig. 6.

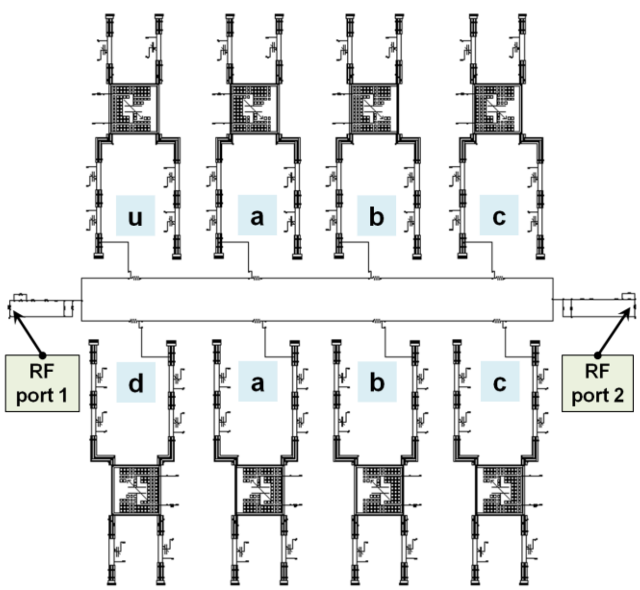

Figure 6: Cadence schematic of the whole RF-MEMS attenuator reported in Fig. 1. The schematic for each of the 8 switches is the same reported in Fig. 2-bottom.

The RF simulation represents the last fundamental step to be taken in order to validate the exploitation of the MEMS compact model library for the simulation of complex RF-MEMS networks.

The network features 8 switches equal to the one reported in Fig. 2-bottom, plus a few passives (resistors, capacitors and inductors) instanced from a standard library in Cadence, and composing lumped element network schemes visible nearby the RF port 1 and 2. Such networks are necessary in order to model the non-idealities occurred because of a technology issue in the vertical transition between the Gold layer of the CPW (CoPlanar Waveguide) structure (see Fig. 1) and the underlying Aluminum buried layer [14]. Such an issue introduces parasitic effects that influence the RF behavior of the network. The qualitative and quantitative extraction of the above-mentioned network is performed according to [13,14].

The network of Fig. 6 is simulated in Spectre (S-parameter simulation up to 30 GHz), and the state of the MEMS switches is reconfigured by applying a DC bias of 0 V (switch/es not-actuated) or 40 V (switch/es actuated). A few simulated attenuation levels are reported in Fig. 7 and compared to the measured S-parameter characteristic.

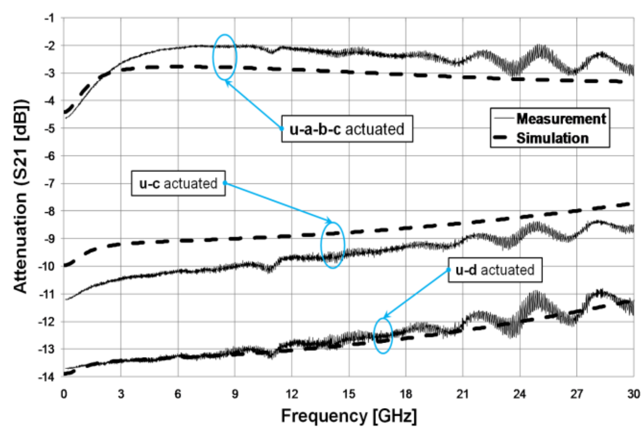

Figure 7: Experimental and simulated characteristic of the S21 parameter (attenuation) for 3 of the 16 possible configurations enabled by the RF-MEMS network of Fig. 1.

The minimum attenuation level is realized by the network when the 3 switching stages (labeled as “a”, “b” and “c” in Fig. 6) are actuated (i.e. resistors shorted) and one of the two branches is selected (in this case switching stage “u” – up actuated [11]). An intermediate attenuation level is realized when the “u” switch is actuated and the resistive stage “c” is shorted. Finally, a higher attenuation level is reached when the “u” – up and “d” – down switching units are activated, and all the resistors are loading the RF line (i.e. none of the “a”, “b” and “c” units are actuated). In this case, the resistive loads are connected in parallel, and the maximum attenuation level can be reached releasing the “u” or the “d” switch [11].

Looking at the plot in Fig. 7 a good agreement of the simulations with the measured S-parameters is observable. In particular, the non-ideal behavior of the Gold to Multi-

Metal transition previously mentioned, introduces a large parasitic series capacitance affecting the S-parameter behavior of the network mainly in the low-frequency range (up to 2-3 GHz) [11,14]. Such a behavior is well predicted by the Spectre simulation, after including in the schematic the aforementioned extracted lumped element network. The difference between measured and simulated results is better than 1 dB in all the analyzed network configurations.

5 CONCLUSIONS

In this work, we discussed the exploitation of a MEMS compact model library, previously implemented by the authors in the VerilogA© programming language, to establish a fast and accurate simulation methodology suitable for predicting the coupled electromechanical and electromagnetic behavior of complex RF-MEMS networks.

We employed as case study a MEMS-based multi-state RF power attenuator comprising a few Poly-Silicon resistors loading the RF line, that can be selected or shorted by controlling cantilever-type MEMS ohmic switches.

First of all, we focused on the electromechanical behavior of the microswitches, reporting the comparison of the measured pull-in/pull-out characteristic with the Spectre© DC simulation of the switch schematic composed with the elemental MEMS models comprised in the software library. The experimental pull-in/pull-out voltage levels are accurately predicted by the simulation.

The RF behavior of the whole MEMS attenuator network was modeled by a schematic in Spectre. It includes microswitches, Poly-Silicon resistors loading the RF line, and extracted lumped element networks accounting for the non-idealities of the technology process. The coupled-field electromechanical and electromagnetic behavior of the sample was simulated in Spectre (S-parameter simulations) for a few of the possible attenuation levels enabled by the MEMS network. The simulated results are in good agreement with the experimental data (difference in the attenuation curves always better than 1 dB up to 30 GHz).

In conclusion, the simulation and modeling approach we propose enables the fast and accurate simulation of the coupled-field behavior of RF-MEMS devices as well as of complex networks, once the employed technology platform is defined and its possible spreads are known.

Such a methodology can constitute a valuable aid for researchers and professionals in the RF-MEMS field, especially in the initial phases of a new device conception. At this stage, indeed, having a tool that enables the fast identification and accurate evaluation of the trade-offs existing among multiple mechanical, electrical and electromagnetic degrees of freedom (dofs), is a significant ease for the work of RF-MEMS designers.

REFERENCES

[1] Y. Zhu, M.R. Yuce and S. Moheimani, "A low-loss MEMS tunable capacitor with movable dielectric," in Proc. of IEEE Sensors Int. Conf., 651-654, 2009.

[2] S. Aliouane, A.B. Kouki and R. Aigner, "RF-MEMS switchable inductors for tunable bandwidth BAW filters," in Proc. of DTIS Int. Conf., 1-6, 2010.

[3] C. D. Patel and G. M. Rebeiz, "RF MEMS Metal-Contact Switches With mN-Contact and Restoring Forces and Low Process Sensitivity," IEEE T-MTT, PP, 1, 2011.

[4] F. Domingue, S. Fouladi and R.R. Mansour, "A reconfigurable impedance matching network using dual-beam MEMS switches for an extended operating frequency range," in Proc. of IEEE MTT Int. Symp., 1552-1555, 2010.

[5] Hao-Han Hsu, A.D. Margomenos and D. Peroulis, "A monolithic RF-MEMS filter with continuously-tunable center-frequency and bandwidth," in Proc. of IEEE SiRF Int. Symp., 169-172, 2011.

[6] S. Gong, H. Shen and N. S. Barker, "A 60-GHz 2-bit Switched-Line Phase Shifter Using SP4T RF-MEMS Switches," IEEE T-MTT, PP, 1, 2011.

[7] King Yuk Chan, R.R. Mansour and R. Ramer, " Miniaturized RF MEMS switch cells for crossbar switch matrices," in Proc. of APMC Int. Conf., 1829-1832, 2010.

[8] H. J. De Los Santos, "RF MEMS Circuit Design for Wireless Communications," Artech House Publishers, 978-15-80533-29-4, 2002.

[9] J. Iannacci, R. Gaddi and A. Gnudi, "Experimental Validation of Mixed Electromechanical and Electromagnetic Modeling of RF-MEMS Devices Within a Standard IC Simulation Environment," IEEE JMEMS, 19, 526-537, 2010.

[10] J. Iannacci, "Mixed-Domain Fast Simulation of RF and Microwave MEMS-based Complex Networks within Standard IC Development Frameworks," Advanced Microwave Circuits and Systems", INTECH, 2010.

[11] J. Iannacci, A. Faes, F. Mastri, D. Masotti, V. Rizzoli, "A MEMS-Based Wide-Band Multi-State Power Attenuator for Radio Frequency and Microwave Applications," in Proc. of NSTI Int. Conf., 328-331, 2010.

[12] G. M. Rebeiz, "RF MEMS: Theory, Design, and Technology," Wiley, 978-04-71201-69-4, 2004.

[13] J. Iannacci and R. Gaddi, "Mixed-Domain Simulation and Wafer-Level Packaging of RF-MEMS Devices," Lambert Academic Publishing, 978-38-38364-21-6, 2010.

[14] J. Iannacci, F. Giacomozzi, S. Colpo, B. Margesin and M. Bartek, "A General Purpose Reconfigurable MEMS-Based Attenuator for Radio Frequency and Microwave Applications," in Proc. of IEEE EUROCON Int. Conf., 1201-1209, 2009.